PHYSICAL REVIEW B **66**, 161304(R) (2002)

Single-hole tunneling into a strain-induced SiGe quantum ring

Jun Liu,[1] A. Zaslavsky,[1,2] B. R. Perkins,[2] C. Aydin,[1] and L. B. Freund[2]
[1]*Department of Physics, Brown University, Providence, Rhode Island 02912*
[2]*Division of Engineering, Brown University, Providence, Rhode Island 02912*
(Received 24 June 2002; revised manuscript received 19 August 2002; published 4 October 2002)

We have observed single-hole tunneling and Coulomb blockade in the resonant tunneling characteristics of an ultrasmall Si/SiGe strained vertical quantum dot. The current steps near the tunneling threshold are due to tunneling of the holes from the emitter to the doubly degenerate ground state of the strain-induced quantum ring in the vertical quantum dot, and the spacing of the steps gives the charging energy of the quantum ring. When a magnetic field is applied parallel to the tunneling direction, the evolution of the single-hole tunneling features reveals a cusp arising from the angular-momentum transition of the single-particle ground state of the quantum ring in the magnetic field.

DOI: 10.1103/PhysRevB.66.161304 PACS number(s): 73.21.La, 73.40.Gk, 73.23.Hk

In analogy to the Aharonov-Bohm effect,[1] closed quantum ring structures possess interesting physical properties due to quantum-mechanical phase coherence and interference, such as energy spectra periodic in the enclosed magnetic flux ϕ with period $\phi_0 = h/e$ and the equilibrium persistent current circling around the ring.[2–5] Both properties have been investigated extensively in various metallic[6,7] and III-V semiconductor quantum rings.[8] Due to recent advances in nanofabrication techniques, cleaner data on the energy spectra of quantum rings have been studied both in a large collection of few-electron quantum rings by optical spectroscopy[9,10] and in a single many-electron quantum ring by transport spectroscopy.[11] In this paper, we report on the energy spectra of the ground state of a single few-hole quantum ring in the magnetic field. The quantum ring arises from the inhomogeneous strain relaxation in strained vertical Si/SiGe pillars.[12–14] Recently, we have used tunneling spectroscopy to observe the predicted periodicity of energy states in the enclosed magnetic flux ϕ, with period ϕ_0 in a single gated vertical quantum dot, which is an unambiguous signature of a quantum ring.[15] Until now, there has been no experimental data on single-hole tunneling into a quantum ring, although a recent report studied single-hole tunneling through electrostatically gated planar Si/SiGe quantum dots.[16] Now, an ultrasmall (diameter $D \sim 45$ nm) strain-induced quantum ring in a vertical quantum dot has a sufficiently large single-carrier charging energy[17,18] to make it possible to investigate the single-particle ground state of the ring when occupied by none or few carriers using resonant tunneling spectroscopy.[11]

Our data come from the magnetotunneling measurements on a *p*-Si/SiGe strained vertical quantum dot with nominal $D = 45$ nm. We have observed single-hole tunneling and Coulomb blockade at the onset of the tunneling, which are due to tunneling of the holes into the spin doublet[18,19] of the ground state of the strain-induced quantum ring in the vertical quantum dot. The magnetotunneling data reflect the single-hole energy spectrum of the quantum ring ground state as a function of the magnetic field parallel to the tunneling direction, and reveal a cusp due to the angular-momentum transition of the single-particle ground state from $l = 0$ to $l = 1$.[10] This angular-momentum transition is the consequence of the competition between the quantum ring potential and the magnetic-field confinement, as discussed below.

The vertical quantum dot was fabricated by electron-beam lithography and reactive ion etching from high-quality strained *p*-Si/SiGe triple-barrier resonant tunneling heterostructure.[20] The nominally undoped triple-barrier region consists of two strained $Si_{0.8}Ge_{0.2}$ quantum wells of widths 35 and 28 Å, separated by a narrow Si middle barrier of width 10 Å and confined by two 35-Å Si barriers. There are 200-Å undoped $Si_{0.8}Ge_{0.2}$ spacer layers graded to p^+-Si contact regions on either side of the active region. Figure 1(a) shows the schematic of the cross section of the device. In contrast to etched III-V semiconductor structures where the sidewall depletion due to Fermi-level pinning at the surface results in the parabolic lateral confinement potential,[8] the Si/SiGe vertical quantum dot that we measured is passivated by silicon dioxide.[14] This results in a much smaller surface density of states that does not cause significant depletion at the sidewall,[21,22] which is manifested by the proper functioning of the 45-nm quantum dot and the approximate proportionality of the tunneling current and the device area in larger Si/SiGe vertical quantum dots fabricated from the same material.

A bias between the top contact and the substrate aligns occupied hole states in the emitter electrode with the quantized hole states in the Si/SiGe quantum wells.[20] Figure 1(b) illustrates the valance band of the active region of the quantum dot in forward bias. Since the 35-Å quantum well is wider than the 28-Å quantum well, the ground state of the coupled quantum wells is mainly localized in the wider well even under modest bias between the emitter and the collector, as shown schematically in Fig. 1(b). In forward bias, the localization of the ground-state wave function in the wider well leads to higher tunneling rate into the wells through the emitter barrier than the tunneling rate out of the well through the collector barrier.[23] Consequently, beyond the current threshold, the occupancy probability of the ground state of the quantum dot is high, and thus the charging effect is significant. Once a hole tunnels in, the second hole must overcome the Coulomb charging energy e^2/C to add into the quantum dot, where C is the total capacitance of the dot. On

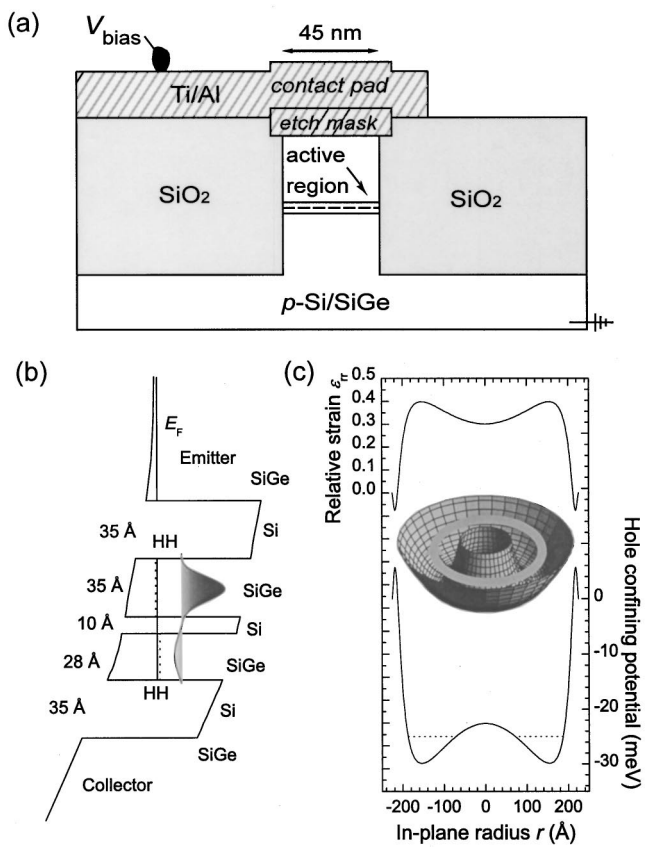

FIG. 1. (a) Schematic of cross section of the vertical quantum dot (not to scale). Hatched regions are metal and the shaded region is silicon dioxide. The bias V is applied between the top contact pad and the p^+-Si substrate. (b) Illustration of the valence band of the active region of the vertical quantum dot in forward bias. The solid line is the lower-lying coupled double quantum well ground state, arising from the heavy-hole ground states that would otherwise exist in isolated SiGe wells of the same width (dashed lines). The wave function is concentrated in the wider well as shown in the graph. (c) Finite element simulation of the strain profile and corresponding strain-induced confining potential in the quantum dot. The top curve shows the calculated radial strain component $\varepsilon_{rr}(r)$ on the midplane of the top 35-Å $Si_{0.8}Ge_{0.2}$ quantum well in the quantum dot (full biaxial strain corresponds to $\varepsilon_{rr}=1$), while the bottom curve is the resulting in-plane hole confining potential as a function of r. The dotted lines mark the ground state of the quantum ring in the ringlike potential near the perimeter, assuming $m^*\sim 0.25m_e$ (see text for details). The inset illustrates the strain-induced quantum ring potential.

the contrary, in reverse bias there is no hole accumulation in the well due to the larger rate tunneling out of the well.[17] As a consequence of the asymmetry of the triple-barrier structure, the tunneling $I(V)$ curve will exhibit strong charging effect in forward bias only, just as in the case of asymmetric double-barrier structures reported in the studies of single-electron charging of quantum dots.[17,24] Figure 1(c) presents the finite element simulation of the in-plane strain profile and the converted potential for holes in the quantum wells.[14,15] The inhomogeneous strain relaxation results in the ringlike high-strain region near the perimeter of the quantum dot, leading to quantum ring confinement as shown in the inset of Fig. 1. The ground state of the quantum dot is confined in the strain-induced quantum ring potential.

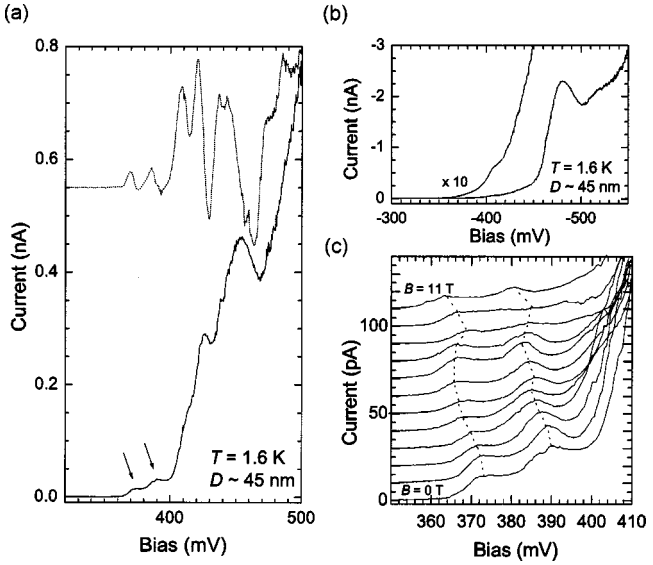

FIG. 2. (a) Resonant tunneling $I(V)$ and dI/dV characteristics at $T=1.6$ K of the vertical quantum dot with a nominal diameter $D=45$ nm in forward bias, showing two current steps at the onset of the tunneling. The current step height is approximately 15 pA. The pairing of the conductance peaks is evident. (b) $I(V)$ and dI/dV characteristics at $T=1.6$ K of the vertical quantum dot in reverse bias. No current steps are observed near the threshold. (c) Evolution of the current steps at the thershold of the forward bias with the magnetic fields from $B=0$ to 11 T at an interval of 1 T. The current-bias curves are offset vertically by 10 pA. Dashed lines are guides to the eye.

Figure 2 shows the $I(V)$ characteristics of the strained vertical quantum dot in both polarities measured at $T=1.6$ K. In forward bias, two current steps at the onset of the tunneling are observed, with the first current step height of $\Delta I\sim 15$ pA, approximately equal to the second current step height. These current steps at the threshold and the single current step height are due to Coulomb blockade through the single-hole charging of the spin doublet ($|\frac{3}{2}, \pm\frac{3}{2}\rangle$) of the ground state. At a higher bias, current starts to flow through the higher-lying hole subbands in the quantum dot, leading to several distinct peaks with higher current. Here we concentrate on the two current steps near the threshold, which reveal the property of the strain-induced quantum ring ground state. The charging energy U can be derived from the first current step width by converting the bias into hole energy using a self-consistent potential calculation. We obtain $U\sim 3.6$ meV. Assuming cylindrical symmetry and taking account of the spatial extension of the quantum ring ground state, the total capacitance of the strain-induced quantum ring can be estimated to be $C\sim C_1+C_2\sim 4.0\times 10^{-17}$ F, using $C_i=\varepsilon\varepsilon_0\pi(r_2^2-r_1^2)/d_i^2$, where r_2 is the outer radius of the ring, r_1 the inner radius of the ring, and d_i the effective barrier thickness. From this we estimate a Coulomb charging energy of $U\sim 4.0$ meV, which is consistent with the measured value. No current steps are observed in reverse bias, as expected.[24]

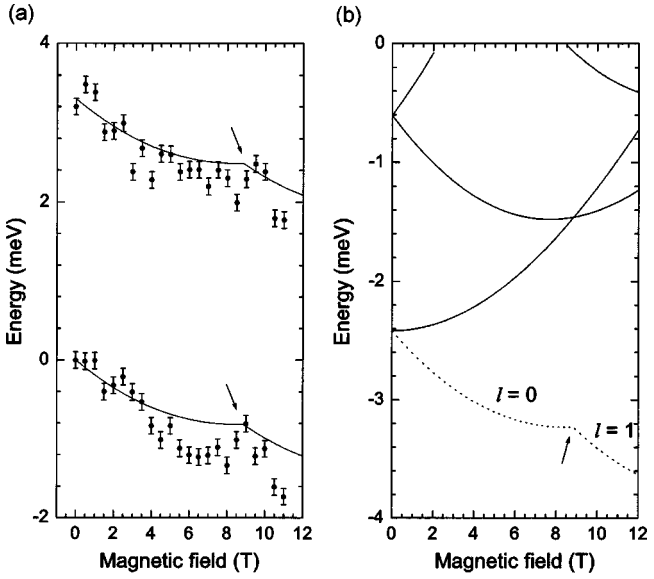

FIG. 3. (a) The energy (relative to the emitter Fermi sea) of the quantized states in the dot corresponding to the two current steps vs the magnetic field, obtained by magnetotunneling spectroscopy at $T=1.6$ K, and separated by a charging energy of $U\sim3.6$ meV. Both energies respond to the magnetic field in a similar way, indicative of tunneling into the spin doublet of the ground state, respectively. A cusp is observed at $B\sim9$ T. The error bars consist of the measurement uncertainties and the uncertainties in the determination of the conductance peaks. The solid lines are the simulated E-B curve, as shown in Fig. 3(b). (b) Numerical simulations of the quantum ring hole states in the magnetic field. The solid line shows the variation of the energy with the magnetic field, relative to the bottom of the quantum wells, while the dotted line shows the energy of quantum ring ground state relative to the emitter Fermi sea in the magnetic field, with the diamagnetic energy included. The cusp at $B\sim9$ T corresponds to the angular-momentum transition of the single-particle ground state of the quantum ring from $l=0$ to $l=1$.

To further verify that the two current steps at the threshold arise from tunneling through the doubly degenerate ground state of the strain-induced quantum ring, we have investigated the device in an external magnetic field B applied parallel to the tunneling current. Figure 2(c) shows the evolution of the current steps at the threshold with the magnetic fields. From the measured tunneling conductance peaks, we can extract the energy of the quantized states in the dot relative to the emitter Fermi sea and plot them with magnetic field as shown in the E-B curve in Fig. 3(a). Both conductance peaks respond to the magnetic field in a similar way, exhibiting an overall shift to lower energy, but with a cusp at around 9 T. The close resemblance of the evolution of both conductance peaks with magnetic fields further indicates that they arise from tunneling into the spin doublet[18] of the ground state, with the same spatial wave function, separated by the charging energy of the quantum dot, $U\sim3.6$ meV. Other contributions to the energy splitting of the ground state could come from the spin-orbit coupling (Rashba effect) and the Zeeman splitting. But only a weak signature of Rashba effect was observed in the heavy-hole system of p-type Si/SiGe quantum wells at very low temperature $T<300$ mK.[25] We measured the magnetotransport at a much larger temperature $T\sim1.6$ K, at which the thermal energy broadening would probably make the spin-orbit coupling unobservable. As for the Zeeman splitting, in a pseudomorphically strained $Si_{0.8}Ge_{0.2}$ layer, the heavy-hole g factor perpendicular to the growth direction can be as high as 4.9,[26] and thus the expected Zeeman splitting energy $g^*\mu_B B$ can be as large as 2.8 meV at $B=10$ T, which is much larger than the temperature broadening at $T=1.6$ K. Nonetheless, we do not observe the Zeeman shifts and the separation between the two conductance peaks remains relatively insensitive to different magnetic fields. This fact can be understood in terms of the conservation of the spin in the tunneling process. The hole states in both the emitter and the quantum wells involved in the tunneling process have similar Zeeman spin splitting and respond to the magnetic field in a correlative way. Thus the Zeeman shifts are unobservable during the tunneling due to the absence of a spin-flip tunneling mechanism.

The cusp in the B dependence of the conductance peaks is reminiscent of the spin singlet-triplet transition of the many-body ground state of a quantum dot,[17–19] but our situation is different. The spin singlet-triplet transition can only happen when an additional hole is added to the quantum dot occupied with one or an odd number of holes in the presence of an external magnetic field. Without the magnetic field, the additional hole would go to the same state as the unpaired hole in the dot, but with the opposite spin, thus forming the spin-singlet state. In a certain magnetic field, the Coulomb repulsion between the two spin-degenerate holes, as well as the exchange interaction and the Zeeman energy, would overcome the energy to redistribute them into different single-particle states, and favor an alignment of their spins to create the spin-triplet state, leading to a feature in the addition energy of the second hole, which is absent in that of the first hole. In our magnetotunneling data, the first conductance peak at the threshold arises from single-hole tunneling into the noninteracting ground state of the empty ring, and thus the hole-hole Coulomb interaction is irrelevant, but it exhibits the same cusp in the E-B curve as the second conductance peak. Accordingly, this peak-to-peak correlation manifests that the cusp is due to the evolution of the single-particle energy level with the magnetic field, and not a signature of the spin singlet-triplet transition. Although the E-B curve of the second conductance peak, corresponding to adding a second hole to the quantum ring, could reveal the spin singlet-triplet transition in principle, we do not observe this effect in our data.

We interpret the cusp to be the consequence of the angular-momentum transition of the single-particle ground state of the strain-induced quantum ring in the magnetic field.[10] We solve the Schrödinger equation numerically with the inhomogeneous-strain-induced potential shown in Fig. 1(c) and the single in-plane effective-mass approximation $m^*\sim0.25m_e$ (Ref. 27) for the lowest coupled subband. Figure 3(b) shows the calculated energies of the quantum ring hole states with the magnetic field, relative to the bottom of the quantum wells, with a cusp at $B\sim9$ T, due to the angular-momentum transition of the single-particle ground

state of the quantum ring from $l=0$ to $l=1$.[10] However, the calculated energy of the quantum ring ground state increases with the applied magnetic field in general, while the measured hole state energies shown in Fig. 3(a) move to lower energies with the magnetic field. This discrepancy arises from the fact that the energies shown in Fig. 3(a) are relative to the Fermi sea in the emitter, whereas the energies of the emitter holes involved in the tunneling increase by the diamagnetic energy in the magnetic field. In the emitter, the large density of holes effectively screens the inhomogeneous-strain-induced potential and the emitter hole states have the same spatial extension as the quantum dot. As a result, the diamagnetic energy of the holes in the emitter is larger than that of the quantum ring ground state confined in the ringlike region. The dotted line in Fig. 3(b) shows the energy of quantum ring ground state relative to the emitter Fermi sea in the magnetic field, with the diamagnetic energy included. The calculated E-B curve is superimposed on the experimental data shown in Fig. 3(a). Agreement is acceptable, given the simplicity of the calculations.

An interesting feature of our ultrasmall ring is the persistent current. In an ideal quantum ring, the persistent current is given by $\partial E/\partial \phi$,[2] which yields $\sim$12 nA from the $E(B)$ data in Fig. 3. A naive semiclassical estimate considering a hole of kinetic energy $\sim$5 meV [Fig. 1(c)] and m^* $\sim 0.25 m_e$ going around a circular orbit of nominal diameter of $\sim$45 nm yields a persistent current of $\sim$90 nA. While the agreement is far from good, given the crudeness of the estimate, the fact that they are of the same order of magnitude is satisfactory.

In conclusion, we have fabricated an ultrasmall vertical strained quantum dot that exhibits single-hole tunneling and Coulomb blockade at the threshold voltage in forward bias. The two current steps at the onset are attributed to tunneling into the doubly degenerate ground state of the strain-induced quantum ring, separated by the charging energy. The single-hole charging enables us to extract the single-particle energy of the quantum ring ground state with different magnetic fields, which exhibits a cusp at $B\sim 9$ T. This cusp is due to the angular-momentum transition from $l=0$ to $l=1$ of the single-particle ground state of the quantum ring in external magnetic fields. This observation is in good agreement with the numerical simulation of the energy spectrum of the inhomogeneous-strain-induced quantum ring.

We appreciate helpful discussions with H. Maris and B. Marston. This work was supported by the NSF MRSEC (Grant No. DMR-0079964). The fabrication facilities were also supported in part by the NSF MRSEC at Brown.

[1] Y. Aharonov and D. Bohm, Phys. Rev. **115**, 485 (1959).
[2] M. Büttiker, Y. Imry, and R. Landauer, Phys. Lett. **96A**, 365 (1983).
[3] R. Landauer and M. Büttiker, Phys. Rev. Lett. **54**, 2049 (1985).
[4] Ho-Fai Cheung, E. K. Riedel, and Y. Gefen, Phys. Rev. Lett. **62**, 587 (1989).
[5] T. Chakraborty and P. Pietiläinen, Phys. Rev. B **50**, 8460 (1994).
[6] L. P. Levy, G. Dolan, J. Dunsmuir, and H. Bouchiat, Phys. Rev. Lett. **64**, 2074 (1990).
[7] V. Chandrasekhar, R. A. Webb, M. J. Brady, M. B. Ketchen, W. J. Gallagher, and A. Kleinsasser, Phys. Rev. Lett. **67**, 3578 (1991).
[8] D. Mailly, C. Chapelier, and A. Benoit, Phys. Rev. Lett. **70**, 2020 (1993).
[9] R. J. Warburton, C. Schäflein, D. Haft, F. Bickel, A. Lorke, K. Karrai, J. M. Garcia, W. Schoenfeld, and P. M. Petroff, Nature (London) **405**, 926 (2000).
[10] A. Lorke, R. J. Luyken, A. O. Govorov, J. P. Kotthaus, J. M. Garcia, and P. M. Petroff, Phys. Rev. Lett. **84**, 2223 (2000).
[11] A. Fuhrer, S. Lüscher, T. Ihn, T. Heinzel, K. Ensslin, W. Wegscheider, and M. Bichler, Nature (London) **413**, 822 (2001).
[12] P. W. Lukey, J. Caro, T. Zijlstra, E. Van der Drift, and S. Radelaar, Phys. Rev. B **57**, 7132 (1998).
[13] H. T. Johnson, L. B. Freund, C. D. Akyüz, and A. Zaslavsky, J. Appl. Phys. **84**, 3714 (1998).
[14] Jun Liu, A. Zaslavsky, C. D. Akyüz, B. R. Perkins, and L. B. Freund, Phys. Rev. B **62**, R7731 (2000).
[15] Jun Liu, A. Zaslavsky, and L. B. Freund, Phys. Rev. Lett. **89**, 096804 (2002).
[16] U. Dötsch, U. Gennser, C. David, G. Dehlinger, D. Grützmacher, T. Heinzel, S. Lüscher, and K. Ensslin, Appl. Phys. Lett. **78**, 341 (2001).
[17] B. Su, V. J. Goldman, and J. E. Cunningham, Science **255**, 313 (1992).
[18] S. Tarucha, D. G. Austing, T. Honda, R. J. van der Hage, and L. P. Kouwenhoven, Phys. Rev. Lett. **77**, 3613 (1996).
[19] S. Lüscher, T. Heinzel, K. Ensslin, W. Wegscheider, and M. Bichler, Phys. Rev. Lett. **86**, 2118 (2001).
[20] C. D. Akyüz, H. T. Johnson, A. Zaslavsky, L. B. Freund, and D. A. Syphers, Phys. Rev. B **60**, 16 597 (1999).
[21] Z. Chen, K. Yasutake, A. Doolittle, and A. Rohatgi, Appl. Phys. Lett. **63**, 2117 (1993).
[22] L. P. Rokhinson, L. J. Guo, S. Y. Chou, and D. C. Tsui, Superlattices Microstruct. **28**, 413 (2000).
[23] T. Schmidt, R. J. Haug, K. V. Klitzing, A. Förster, and H. Lüth, Phys. Rev. Lett. **78**, 1544 (1997).
[24] M. Tewordt, L. M. Moreno, J. T. Nicholls, M. Pepper, M. J. Kelly, V. J. Law, D. A. Ritchie, J. E. F. Frost, and G. A. C. Jones, Phys. Rev. B **45**, 14 407 (1992).
[25] V. Senz, T. Heinzel, T. Ihn, K. Ensslin, G. Dehlinger, D. Grützmacher, and U. Gennser, Phys. Rev. B **61**, R5082 (2000).
[26] F. F. Fang, P. J. Wang, B. S. Meyerson, J. J. Nocera, and K. Ismail, Surf. Sci. **263**, 175 (1992).
[27] We use the six-band Luttinger-Kohn model to calculate the in-plane effective-mass m^* of the lowest hole subband in our coupled Si/SiGe double quantum wells, see J. M. Luttinger and W. Kohn, Phys. Rev. **97**, 869 (1955).